We are IntechOpen, the world's leading publisher of Open Access books Built by scientists, for scientists

6,900
Open access books available

185,000
International authors and editors

200M
Downloads

Our authors are among the

154
Countries delivered to

TOP 1%
most cited scientists

12.2%
Contributors from top 500 universities



WEB OF SCIENCE™

Selection of our books indexed in the Book Citation Index in Web of Science™ Core Collection (BKCI)

Interested in publishing with us?
Contact book.department@intechopen.com

Numbers displayed above are based on latest data collected.
For more information visit www.intechopen.com



19

Inner Filter Effect in the Fluorescence Emission Spectra of Room Temperature Ionic Liquids with-β-Carotene

Krzysztof Pawlak[1], Andrzej Skrzypczak[2] and Grazyna E. Bialek-Bylka[1]
[1]*Institute of Physics, Faculty of Technical Physics,*
[2]*Faculty of Chemical Technology,*
Poznan University of Technology,
Poland

1. Introduction

Steady-state fluorescence spectroscopy is highly sensitive an analytical fluorescence detecting tool limited to diluted samples. The serious problem of quantitative analysis is dominant in the samples with optical density higher than 0.05 (10 mm cell) detected in the right angle cell geometry, because of the two kinds of inner filter effects IFEs (Lakowicz, 2006; Li & Hu, 2007; Kao et al., 1998). The primary inner filter effect (PIFE) - defined as the decrease in the intensity of the excitation beam at the point of observation because of the chromophore optical absorption in the excitation region. In the fluorescence emission experiment, an apparent decrease in the fluorescence emission quantum yield and/or distortion of band shape as a result of re-absorption of emitted radiation is observed. Finally, some molecules of the investigated samples will be excited by the less intense light. For example the excitation light intensity (I_o) at center of 10 mm cuvette is (0.88 I_o) for (OD = 0.1). The secondary inner filter effect (SIFE) takes place when the fluorescence intensity decreases as a result of the chromophore absorption in the emission region. More serious is PIFE than SIFE because excitation wavelengths are always shorter than emission wavelength, especially in organic samples. Generally, the relationship between fluorescence intensity (I_F) and fluorophore concentration (c) is logarithmic (Guilbault, 1990) - $I_F = I_o \phi_F (1-e^{-\varepsilon l c})$, where ($I_o$) is the incident light intensity, (ϕ_F) is the fluorescence quantum efficiency, (ε) is the molar extinction coefficient, (l) is the cell path length. In the concentrated sample the excitation radiation is absorbed significantly by the fluorophore or other chromophores in the cell and the (PIFE) plays a significant role.

For dilute solutions (absorbance <0.01) fluorescence is uniformly distributed. The above equation is reduced to the linear form: $I_F = k\, I_o\, \phi_F\, \varepsilon\, l\, c$ with approximately 1% error, where (k) is proportionality constant. For the fluorescence experiment it is always important to establish either by calculation or by measurement the concentration value (C_{max}) at which a plot of fluorescence emission against concentration becomes nonlinear. This value can be calculated from equation: $C_{max} = 0.05/\varepsilon\, l$, where: symbols ($\varepsilon$) and (l) have the same meaning as in the other equations. From the nonlinear calibration curves (fluorescence intensity *versus* fluorophore concentrations) the information of the presence of the IFEs in

concentrated samples can be found. The fluorescence data (calibration curve) of high molecule concentrations (10 mm cuvette) can be corrected for IFE (Lakowicz, 1983): $F_{corr} = F_{obs}$ Antilog$(A_{ex} + A_{em})/2$ where: (F_{obs}) and (F_{corr}) - the observed and corrected fluorescence intensity values, respectively and (A_{ex}) and (A_{em}) - the absorbance values at the excitation and the emission wavelengths, respectively. If calibration curve is not perfectly linear, it means that the molar extinction coefficient (ε) depends on the refractive index (n) of the solvent: $n\,\varepsilon / (n^2 + 2)^{1/2}$.

In order to be able to measure the IFE - less fluorescence spectra of RTILs alone and with non-polar (very low fluorescence yield in conventional solvent like hexane) β-carotene molecules in RTILs, a special quartz Suprasil μ-cuvette has been used. Short pass cells are designed in order to reduce the PIFE along a particular (usually excitation) axis (Koel, 2008; Wasserscheid & Welton, 2008).

According to our knowledge the IFE study of strongly fluorescing RTILs alone and with β-carotene has not been undertaken yet, but they are very important data for fluorescence result discussion. Generally, both the fluorescence emission or excitation spectra can be measured, but in our project we concentrated on the measurement of the emission spectra, because of the less subject to IFE than in fluorescence excitation spectra. The less dependence on IFE fluorescence excitation spectra will be discuss in order to explain 'red edge effect'.

2. Room temperature ionic liquids - synthesis and purification

The following designed structures of RTILs were synthesized and carefully purified: 1-methyl-3-octyloxymethylimidazolium tetrafluoroborate (*IL1*), 1-methyl-3-hexyloxymethylimidazolium bis(trifluoromethylsulfonyl)imide (*IL2*), 1-methyl-3-octyloxymethylimidazolium bis(trifluoromethylsulfonyl)imide (*IL3*) and 1-methyl-3-octylimidazolium tetrafluoroborate (*IL4*). The (*IL2*) and (*IL3*) RTILs differ in the cationic part $[C_6H_{13}OCH_2\text{-}C_1Im]^+$, $[C_8H_{17}OCH_2\text{-}C_1Im]^+$, respectively. According to the literature (Koel, 2008; Wasserscheid & Welton, 2008) and our measurements viscosity of tested compounds increased due to the cations: $[C_6H_{13}OCH_2\text{-}C_1Im]^+$, $[C_8H_{17}OCH_2\text{-}C_1Im]^+$ and $[C_8\text{-}C_1Im]^+$. The (*IL3*) and (*IL1*) RTILs have the same cationic part: $[C_8H_{17}OCH_2\text{-}C_1Im]^+$ but different anions $[(CF_3SO_2)_2N]^-$ and $[BF_4]^-$, respectively. The (*IL1*) and (*IL4*) RTILs having the same anion $[BF_4]^-$ differ in the cationic part: $[C_8H_{17}OCH_2\text{-}C_1Im]^+$ and $[C_8\text{-}C_1Im]^+$, respectively.

The ionic liquid 1-methyl-3-octylimidazolium tetrafluoroborate was purchased from the Sigma-Aldrich and carefully purified.

2.1 Preparation of testing ILs

Preparation of 1-methyl-3-octyloxymethylimidazolium and 1-methyl-3-hexyloxymethyl-imidazolium chlorides (Fig. 1.). To anhydrous solution of 0.1 mol 1-methylimidazole in acetonitrile, 0.105 mol of chloromethyloctyl ether or chloromethylhexyl ether was added. The reaction was carried out for 1h and the product was purified by extraction with heptane in 343K. The final product was hygroscopic compound with the yield 92.5% for 1-methyl-3-octyloxymethylimidazolium chloride and 93.2% for 1-methyl-3-hexyloxymethyl-imidazolium chloride.

Preparation of 1-methyl-3-octyloxymethylimidazolium tetrafluoroborate (*IL1*) (Fig. 2) (Pernak et al., 2001) and 1-methyl-3-octyloxymethylimidazolium bis(trifluoromethylsulfonyl)imide (*IL3*), and 1-methyl-3-hexyloxymethylimidazolium bis(trifluoromethylsulfonyl)imide (*IL 2*).

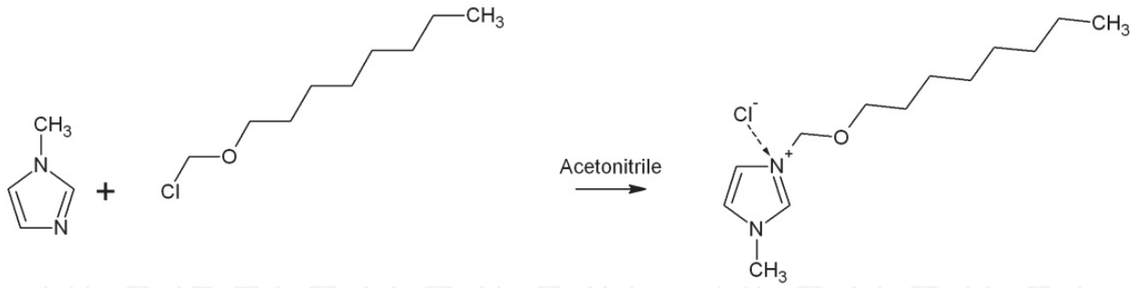


Fig. 1. Preparation of 1-methyl-3-octyloxymethylimidazolium chloride.

To 1-methyl-3-octyloxymethylimidazolium chloride or 1-methyl-3-hexyloxymethyl-imidazolium chloride (0.09 mol) dissolved in 30 ml methanol, sodium tetrafluoroborate (0.095 mol) or lithium bis(trifluoromethylsulfonyl)imide was added. The reaction was completed by heating (at 328K) on a water bath with stirring (24 h). After removing solvent in vacuum, product was once again dissolved in anhydrous acetone in order to filter small amounts of NaCl and excess of $NaBF_4$ or $Li[(CF_3SO_2)_2N]$. Products were a colorless liquids with the yield of 98%.

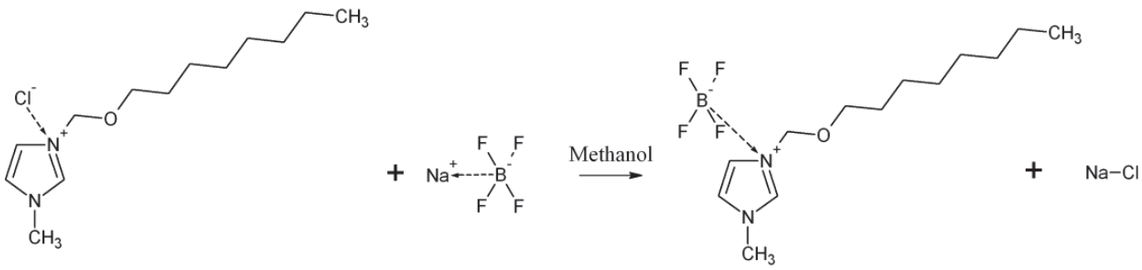
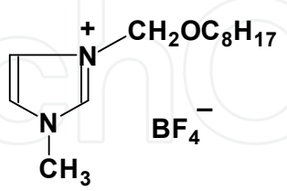


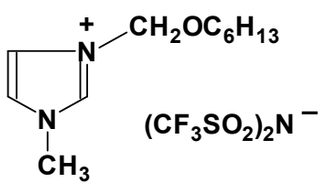
Fig. 2. Preparation of 1-methyl-3-octyloxymethylimidazolium tetrafluoroborate (IL1).

2.2 Structures of synthesized and tested ionic liquids

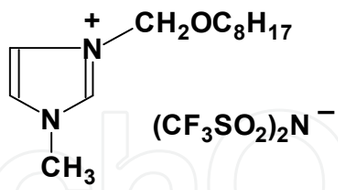
(*IL1*), $[C_8H_{17}OCH_2\text{-}C_1Im][BF_4]$, 1-methyl-3-octyloxymethylimidazolium tetrafluoroborate:



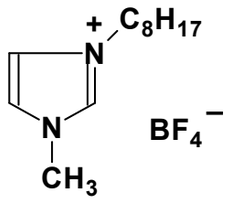
(*IL2*), $[C_6H_{13}OCH_2\text{-}C_1Im][(CF_3SO_2)_2N]$, 1-methyl-3-hexyloxymethylimidazolium bis(trifluoromethylsulfonyl)imide:



(*IL3*), $[C_8H_{17}OCH_2\text{-}C_1Im][(CF_3SO_2)_2N]$, 1-methyl-3-octyloxymethylimidazolium bis(trifluoromethylsulfonyl)imide:



(*IL4*), $[C_8\text{-}C_1Im][BF_4]$, 1-methyl-3-octylimidazolium tetrafluoroborate:



2.3 Purification of testing ILs

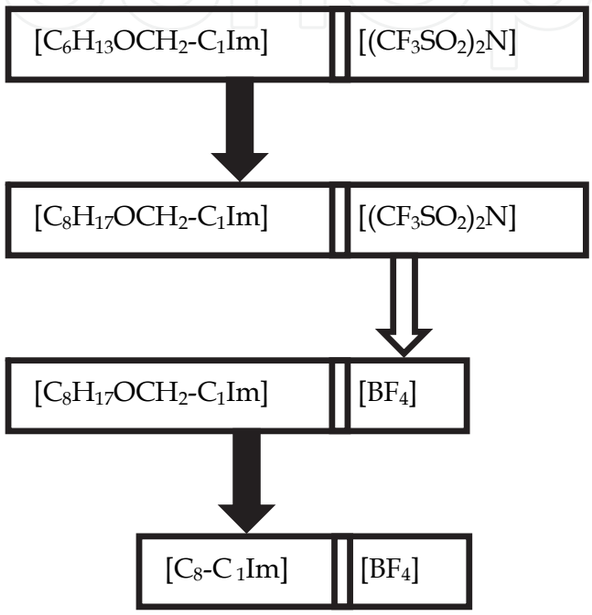
It is well known that ILs should be colorless, but frequently they are not. Chromophores which are present in ionic liquids are the products of side reactions occurring at high temperatures (higher than 75^0C) especially in the alkylation reactions when ILs halides are made (Earle et al. 2007). Our attempt to have "spectroscopic grade" ILs was done in four ways (Gordon et al., 2003):

1. purification of started materials - all substrates were distilled just before reactions,
2. control temperature of quaternisation reactions – temp. below 50^0C,
3. controlling conditions of anion exchange,
4. cleaning of ILs – passing dichloromethane solution of IL (3:1) through the special column, similar to the one used in conventional chromatography. Column was packed with charcoal and Celite and pretreated with dichloromethane.

2.4 Experimental system and spectroscopic methods

The aim of this chapter also is the introduction of the photo physical study of model system (β-carotene in RTILs) mimicking very well spectroscopic data of this photosynthetic pigment *in situ* in the photosynthetic system. Unique fluorescence properties of β-carotene in room temperature ionic liquids (RTIL) (Bialek-Bylka et al., 2007) and new (β-carotene) electronic states ($3A_g^-$ and $1B_u^-$) of both important in photosynthesis isomers: all-*trans* and 15-*cis* in ionic liquid with dimethylformamide (DMF) were found (Bialek-Bylka et al., 2008) and also a sensor detecting the methoxy group in the cation part of imidazolium ionic liquid was developed by us (Pawlak et al., 2009). In order to determine a detailed answer to the unique fluorescence properties, around 100 times higher fluorescence yield of β-carotene in (*IL1*) (1-methyl-3-octyloxymethylimidazolium tetrafluoroborate) than in standard solvent *n*-hexane, the designed structures of RTILs were synthesized and carefully purified: 1-methyl-3-octyloxymethylimidazolium tetrafluoroborate (*IL1*), 1-methyl-3-hexyloxymethylimidazolium bis(trifluoromethylsulfonyl)imide (*IL2*), 1-methyl-3-octyloxymethylimidazolium bis(trifluoromethylsulfonyl)imide (*IL3*), 1-methyl-3-

octylimidazolium tetrafluoroborate (*IL4*). The differences in the structures of the cationic and anionic part of the RTILs investigated by us are shown in the Scheme 1. In this scheme: the first (*IL2*) and second (*IL3*) RTILs differ in the cationic part $[C_6H_{13}OCH_2\text{-}C_1Im]^+$, $[C_8H_{17}OCH_2\text{-}C_1Im]^+$, respectively. According to the literature (Koel, 2008; Wasserscheid & Welton, 2008) and our measurements viscosity of tested compounds increased due to the cations: $[C_6H_{13}OCH_2\text{-}C_1Im]^+$, $[C_8H_{17}OCH_2\text{-}C_1Im]^+$ and $[C_8\text{-}C_1Im]^+$. The second (*IL3*) and third (*IL1*) RTILs have the same cationic part: $[C_8H_{17}OCH_2\text{-}C_1Im]^+$. Finally third (*IL1*) and fourth (*IL4*) RTILs differ again in the cationic part: $[C_8H_{17}OCH_2\text{-}C_1Im]^+$ and $[C_8\text{-}C_1Im]^+$, respectively, but having the same anion $[BF_4]^-$.



Scheme 1. The differences in the structure of the cationic and anionic part of the investigated RTILs: $[C_8H_{17}OCH_2\text{-}C_1Im][BF_4]$, (1-methyl-3-octyloxymethylimidazolium tetrafluoroborate) (*IL1*); $[C_6H_{13}OCH_2\text{-}C_1Im][(CF_3SO_2)_2N]$, (1-methyl-3-hexyloxymethylimidazolium bis(trifluoromethylsulfonyl) imide) (*IL2*); $[C_8H_{17}OCH_2\text{-}C_1Im][(CF_3SO_2)_2N]$, (1-methyl-3-octyloxymethylimidazolium bis(trifluoromethylsulfonyl)imide) (*IL3*); $[C_8\text{-}C_1Im][BF_4]$, (1-methyl-3-octylimidazolium tetrafluoroborate) (*IL4*).

In order to be able to measure the IFE - less fluorescence spectra of RTILs alone and with non-polar and almost non-fluorescing β-carotene molecules in RTILs, a special quartz Suprasil μ-cuvette (1 mm x 10 mm) was used. Short pass cell is used in order to reduce the PIFE along a particular (usually excitation) axis (Koel, 2008; Wasserscheid & Welton, 2008). Generally, the fluorescence emission or excitation spectra can be measured. For our project we concentrated on measurement of the emission spectra because they are less subject to IFE than fluorescence excitation spectra.

The ultraviolet (UV) and visible (Vis) absorption and fluorescence spectra were measured with UV-VIS Lambda 20 Perkin-Elmer Spectrophotometer and LS-55 Perkin-Elmer fluorescence spectrometer, respectively. Both fluorescence quartz cuvettes: a standard square 10 mm x 10 mm and a short path (μ-cuvette) 1 mm x 10 mm, were used. The right angle fluorescence measurements geometry is shown in the Fig. 3.

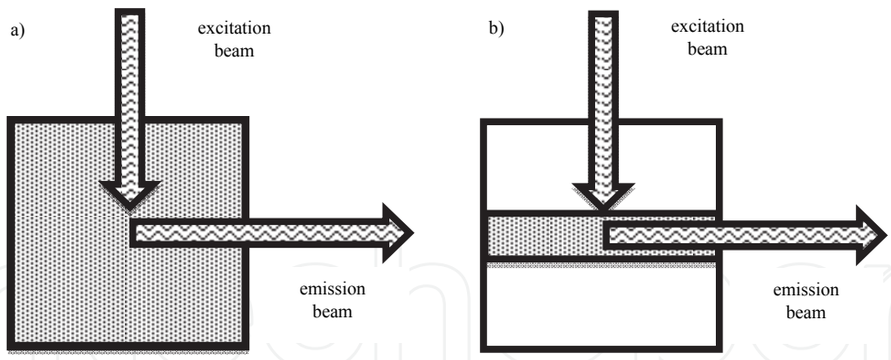


Fig. 3. The right angle cell geometry of the fluorescence measurements: a) standard cuvette 10 mm x 10 mm, b) μ- cuvette 1 mm x 10 mm.

Fluorescence quantum yield was calculated according to the formula (Albani, 2007):

$$Q_x = Q_r \frac{A_r}{A_x} \frac{\int_0^\infty F_x d\lambda}{\int_0^\infty F_r d\lambda} \frac{n_x^2}{n_r^2} \tag{1}$$

where: (Q_x) and (Q_r) are the fluorescence quantum yields of measured sample (x) and reference (r) (Coumarin 6-$C_{20}H_{18}N_2O_2S$; 98%; Sigma-Aldrich), respectively; $\int_0^\infty F d\lambda$ are areas under the fluorescence spectra of the sample (F_x) and the reference (F_r), respectively; (A_x) and (A_r) are the optical densities of the sample and the reference solution at the excitation wavelength, respectively; and (n_x) and (n_r) are the values of the refractive index for the sample and reference, respectively.

3. Results and discussion

In this chapter the attempt in order to explain the unusual high fluorescence quantum yield of β-carotene in RTILs has been undertaken. The inner-filter effect in fluorescence spectra has been observed in a conventional right angle cell. In order to minimize this effect a short pass cell (μ-cuvette) was applied. The right angle geometry is the most common in the spectroscopy, because at right an angle the elastic light scattering signal is the least intense. Also the cell walls directly illuminated by the excitation beam are not directly viewed, so the contribution of fluorescence cell wall distortion is reduced (Ingle & Crouch, 1988). Application of the RTILs as solvents for photo physical studies of molecules in RTILs (in our case photosynthetic pigment all-*trans* β-carotene) depends on transparency of solvents in the visible region of absorption.

Figure 4 shows the absorption spectra of synthesized ionic liquids. These ionic liquids are characterized by a spectral purity in the range above 350 nm. Comparison of these spectra and literature data (Paul & Samanta, 2006) has shown that our ionic liquid purification technique is very efficient.

The figure 5 presents normalized absorption spectra of all-*trans* β-carotene in the following RTILs: *(IL1)*, *(IL2)*, *(IL3)*, *(IL4)*.

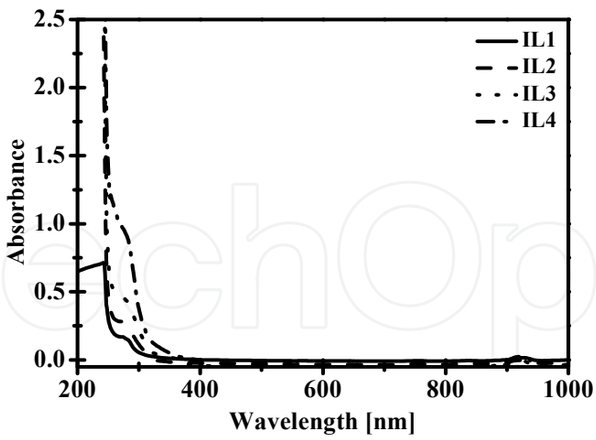


Fig. 4. The absorption spectra of *(IL1)* $[C_8H_{17}OCH_2\text{-}C_1Im][BF_4]$; *(IL2)* $[C_6H_{13}OCH_2\text{-}C_1Im][(CF_3SO_2)_2N]$; *(IL3)* $[C_8H_{17}OCH_2\text{-}C_1Im][(CF_3SO_2)_2N]$; *(IL4)* $[C_8\text{-}C_1Im][BF_4]$ in μ-cuvette.

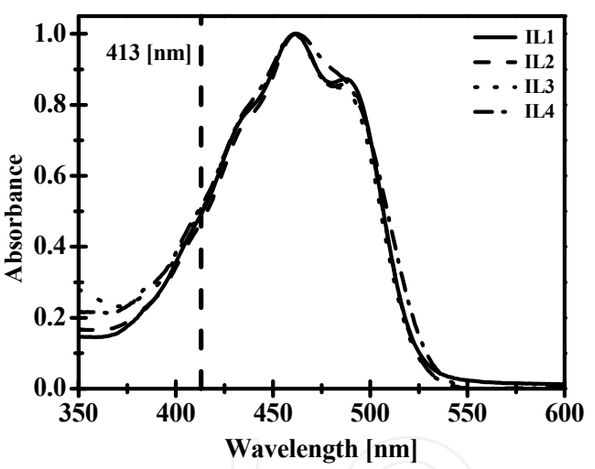


Fig. 5. Normalized absorption spectra of all-*trans* β-carotene in *(IL1)* $[C_8H_{17}OCH_2\text{-}C_1Im][BF_4]$; *(IL2)* $[C_6H_{13}OCH_2\text{-}C_1Im][(CF_3SO_2)_2N]$; *(IL3)* $[C_8H_{17}OCH_2\text{-}C_1Im][(CF_3SO_2)_2N]$; *(IL4)* $[C_8\text{-}C_1Im][BF_4]$; T = 298K; 413 nm is the excitation wavelength used for the fluorescence emission spectra.

The fluorescence emission spectra of all-*trans* β-carotene in RTILs: 1-methyl-3-octyloxymethylimidazolium tetrafluoroborate *(IL1)*, 1-methyl-3-hexyloxymethylimidazolium bis(trifluoromethylsulfonyl)imide *(IL2)*, 1-methyl-3-octyloxymethylimidazolium bis(trifluoromethylsulfonyl)imide *(IL3)* and 1-methyl-3-octylimidazolium tetrafluoroborate *(IL4)* in standard cuvette and in μ-cuvette are shown in Figure 6 (A-D).

The comparison of the RTIL fluorescence spectra measured in both cells (regular and micro) shows the so called 'red tail' (Paul & Samanta, 2006) especially in a case of (*IL2*) and (*IL3*). This effect can be eliminated to high extend in all samples except (*IL4*) where practically

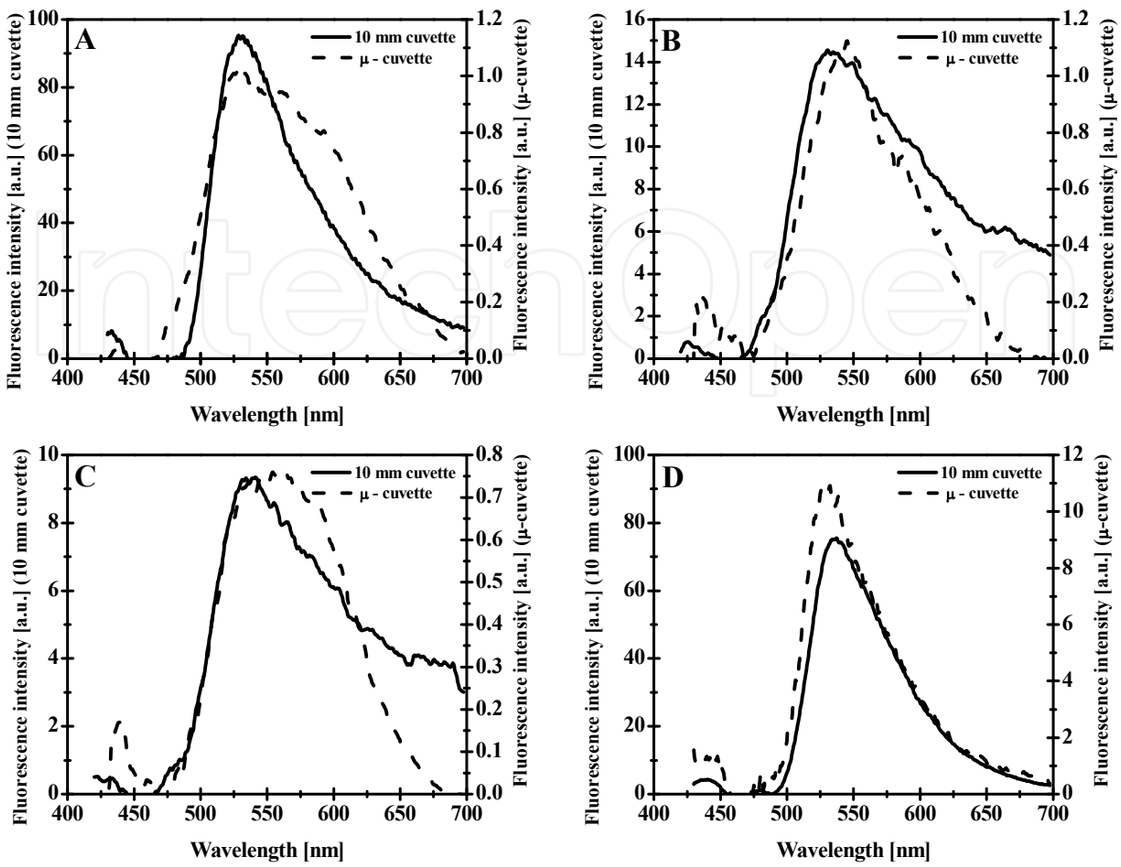


Fig. 6. The fluorescence emission spectra of all-*trans* β-carotene (5 μM) in: (A)- (*IL1*), $[C_8H_{17}OCH_2\text{-}C_1Im][BF_4]$; (B)- (*IL2*), $[C_6H_{13}OCH_2\text{-}C_1Im][(CF_3SO_2)_2N]$; (C)- (*IL3*), $[C_8H_{17}OCH_2\text{-}C_1Im][(CF_3SO_2)_2N]$; (D)- (*IL4*), $[C_8\text{-}C_1Im][BF_4]$ in the standard cuvette and in the μ-cuvette; λ_{ex} = 413 [nm].

such effect does not exist. The maxima of the fluorescence emission spectra of β-carotene in the investigated RTILs are at around 530 nm. Quenching of the fluorescence intensity of RTILs by β-carotene is not linear with path length of the cell (changing from regular -10 mm to micro cell -1 mm).

The fluorescence emission spectra of the ionic liquids: (*IL1*), 1-methyl-3-octyloxymethylimidazolium tetrafluoroborate; (*IL2*), 1-methyl-3-hexyloxymethylimidazolium bis(trifluoromethylsulfonyl)imide; (*IL3*), 1-methyl-3-octyloxymethylimidazolium bis(trifluoromethylsulfonyl)imide and (*IL4*), 1-methyl-3-octylimidazolium tetrafluoroborate in the standard and μ-cuvette are shown in Figure 7 (A-D).

The values of fluorescence intensities of RTIL spectra differ considerably with RTIL structure. For investigated samples these values in [a. u.] are: 341.0, 45.0, 26.6, 942.6 in 10 mm standard cuvette and 5.4, 7.4, 4.6, 203.9 in μ–cuvette. There is different 'red tail' effect in the fluorescence emission spectra of RTILs. The most pronounce effect is in a case of (*IL4*) but in a sample of β-carotene in (*IL4*) practically there is no such effect. The fluorescence intensity of RTILs is quenched by β-carotene. This effect one can see by comparison of the

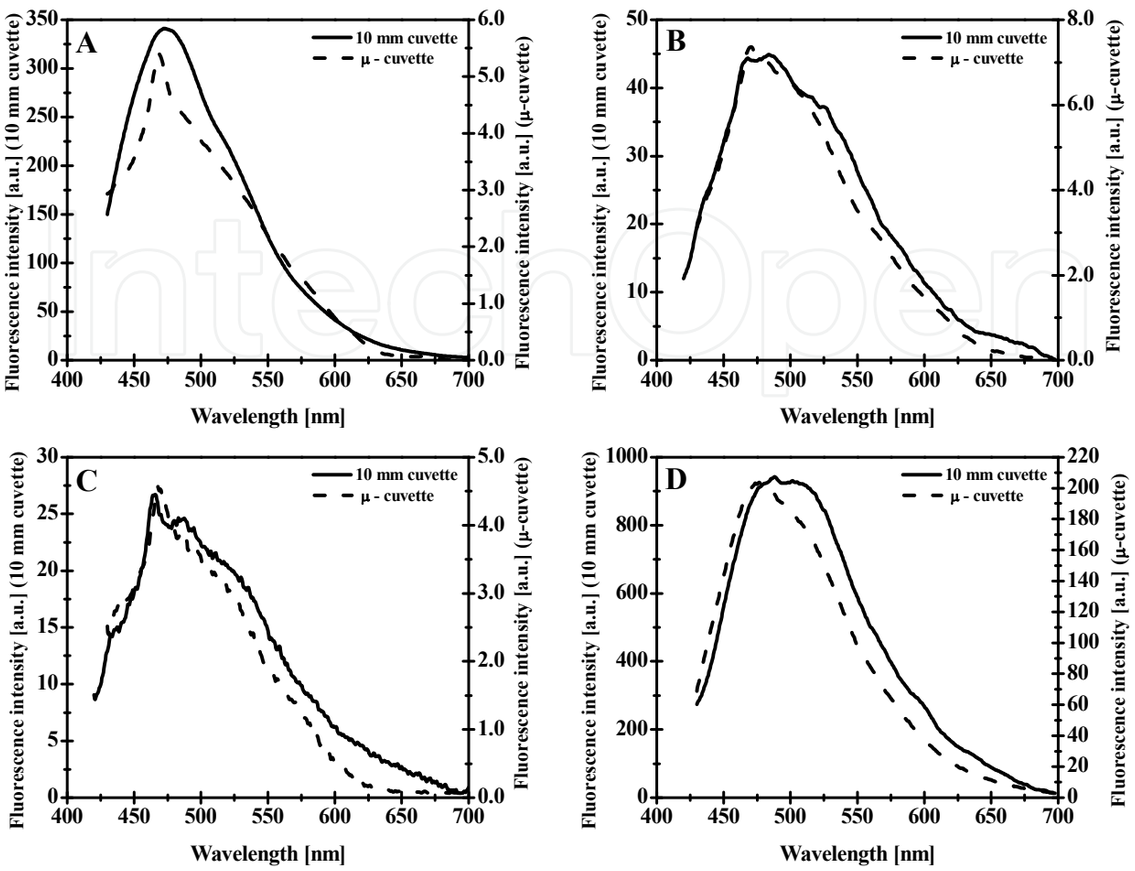


Fig. 7. The fluorescence emission spectra of: (A)- (*IL1*) $[C_8H_{17}OCH_2\text{-}C_1Im][BF_4]$; (B)- (*IL2*) $[C_6H_{13}OCH_2\text{-}C_1Im][(CF_3SO_2)_2N]$; (C)- (*IL3*) $[C_8H_{17}OCH_2\text{-}C_1Im][(CF_3SO_2)_2N]$; (D)- (*IL4*) $[C_8\text{-}C_1Im][BF_4]$ in the standard cuvette and μ-cuvette; λ_{ex} = 413 [nm].

set of Figure 6 (A-D) and Figure 7 (A-D). For spectroscopic details see Table 1. The β-carotene quenching of RTIL fluorescence is at the same level in a case of (*IL2*) and (*IL3*). The highest effect of β-carotene fluorescence quenching of RTIL in 10 mm cell is for (*IL4*) but the lowest for (*IL1*).

The analysis of all RTIL fluorescence data (Table 1) shows that the half band width $\lambda_{1/2}$ is constant within the experimental error ± 2 nm in a case of measurement in micro cell. But this values ($\lambda_{1/2}$) are bigger for β-carotene in RTILs with longer chain as we can see from comparison of (IL4) and (IL1); and also (IL2) and (IL3). The wavelength at the fluorescence maximum (λ_{max}) in the micro cell measurement is 530 nm for β-carotene in (IL1) and (IL4) (both with an anion $[BF_4]^-$). But for (IL2) and (IL3) (with an anion $[(CF_3SO_2)_2N]^-$) the (λ_{max}) is shifted towards longer wavelengths 543 nm and 554 nm in a case of shorter (IL2) chain, and longer (IL3) chain, respectively. In a case of fluorescence measurement in standard cuvette such relation is not observed.

The all-*trans* β-carotene fluorescence yield (ϕ_F = 1.96 ± 0.03) in ionic liquid (1-methyl-3-octyloxymethylimidazolium tetrafluoroborate) according to our previous study (Bialek-Bylka, 2007) is around hundred times higher than in standard solvent (*n*-hexane). The excitation wavelength at 413 nm was selected in order to excite both RTILs alone and β-

standard or μ- cuvette			IL1	IL2	IL3	IL4
β-carotene in RTILs	λ_{max} ± 1 [nm]	Standard	528	530	534	537
		Micro	530	543	554	530
		$\Delta\lambda_{max}$	-2	-13	-20	7
	F_{max} ± 0.1	Standard	95.3	14.5	9.3	75.5
		Micro	1.1	1.1	0.7	10.9
	$\lambda_{1/2}$ ± 2 [nm]	Standard	80	126	127	73
		Micro	123	96	117	68
		$\Delta\lambda_{1/2}$	-43	30	10	5
RTILs	λ_{max} ± 1 [nm]	Stand.	473	483	464	488
		Micro	468	470	467	479
		$\Delta\lambda_{max}$	5	13	-3	-9
	F_{max} ± 0.1	Standard	341.0	45.0	26.6	942.6
		Micro	5.4	7.4	4.6	203.9
	$\lambda_{1/2}$ ± 2 [nm]	Standard	103	129	125	119
		Micro	107	107	109	110
		$\Delta\lambda_{1/2}$	-4	22	16	9
	F_{max} RTIL/ β-car	Standard	3.6	3.1	2.9	12.5
	F_{max} RTIL/ β-car	Micro	4.9	6.7	6.6	18.7

(*IL1*) $[C_8H_{17}OCH_2\text{-}C_1Im][BF_4]$ (*IL2*) $[C_6H_{13}OCH_2\text{-}C_1Im][(CF_3SO_2)_2N]$
(*IL3*) $[C_8H_{17}OCH_2\text{-}C_1Im][(CF_3SO_2)_2N]$ (*IL4*) $[C_8\text{-}C_1Im][BF_4]$

Table 1. The spectroscopic parameters of RTILs and β-carotene in RTILs.

carotene in RTILs. The quantum yield (ϕ_F) of β-carotene in RTILs is much lower than (ϕ_F) of only RTILs. The values of quantum yields (ϕ_F) of β-carotene in RTILs and RTILs alone are listed in Table 2.

Since the fluorescence efficiency of RTILs is sensitive to the excitation wavelength, the fluorescence quantum yield is also dependent on the excitation wavelength. The fluorescence quantum yield of RTILs and β-carotene in RTILs (Table 2) was estimated for excitation wavelength 413 nm at room temperature; as reference sample Coumarin was used.

The polarity of the most imidazolium ionic liquids lies between that of acetonitrile and methanol and is comparable to the short chain alcohols (Mandal et al., 2006).

RTILs	ϕ_F (%) RTILs	ϕ_F (%) β-carotene in RTILs	n ± 0.001
(IL1) $[C_8H_{17}OCH_2\text{-}C_1Im][BF_4]$	1.009 ± 0.005	0.034 ± 0.002	1.433
(IL2) $[C_6H_{13}OCH_2\text{-}C_1Im][(CF_3SO_2)_2N]$	2.628 ± 0.027	0.03 ± 0.01	1.433
(IL3) $[C_8H_{17}OCH_2\text{-}C_1Im][(CF_3SO_2)_2N]$	3.044 ± 0.015	0.026 ± 0.003	1.431
(IL4) $[C_8\text{-}C_1Im][BF_4]$	6.26 ± 0.63	0.26 ± 0.05	1.432

Table 2. The fluorescence quantum yield (ϕ_F) and refractive index (n) of RTILs.

The ionic liquid viscosity change effect was obtained by the bipolar solvent (DMF). Influence of the ionic liquid viscosity has been detected by the fluorescence emission and absorption spectra. Important information is that the new electronic states of β-carotene were found in the mixture of RTIL and DMF (Bialek-Bylka, 2008).

In the Figure 8 (B1) the fluorescence maxima of different concentrations of RTIL in DMF are at shorter wavelength at around 475 nm but bands around 525 nm belong to the fluorescence of all-*trans* β-carotene in RTIL. The λ_{ex} at 413 nm was selected in order to give an opportunity for excitation of both the all-*trans* β-carotene in RTILs and only the RTILs.

The ionic liquid fluorescence signal of RTILs is quenched by β-carotene. The Figure 8 (A1) shows the fluorescence spectra (λ_{ex} = 413 nm) of binary solvent (*IL4*, $[C_8\text{-}C_1Im][BF_4]$ + DMF) with different concentration of RTIL. The 'pure' (corrected for fluorescence intensity of ionic liquids) spectra of all-*trans* β-carotene in binary solvent with different concentration of RTIL in DMF; λ_{ex} = 413 nm; concentration of β-carotene 5 μmol are shown in Figure 8 (C1). The spectra (Fig. 8 (A1)) can be resolved into two Gaussian components: short and long wavelength. In the literature (Paul & Samanta, 2006) also two components were reported in the case of imidazolium based RTILs. Authors assigned the short wavelength component to unassociated imidazolium ion and the long wavelength component to various associated forms of the imidazolium ion. These associated species (stacked dimers and oligomers of the imidazolium ions) are responsible (Paul & Samanta, 2006) for the unique absorption and fluorescence of the imidazolium RTILs.

Figure 8 (C1) shows the highest intensity of the fluorescence of β-carotene in a case of pure (100%) RTIL (*IL4*). The fluorescence intensities of only RTIL (Figure 8 (A1)) and β-carotene in RTIL (Figure 8 (B1)) are different (for example for 100% ionic liquid: 221 [a. u.] and 63 [a. u.], respectively). There exists quenching of RTIL fluorescence by β-carotene molecule in this system.

The fluorescence emission intensity of (*IL4*) (Figure 9 A) and all-*trans* β-carotene in (*IL4*), $[C_8\text{-}C_1Im][BF_4]$ increases nonlinearly with concentration of RTIL (Figure 9 B). The three linear phases are present in both Figures 9 A and B.

The explanation of the parameters of the curves: a, b and c of Figures 9 (A-D) is in Table 3.

Absorption measurement sensitivity of the spectrometer is limited by the ability of the instrument to discriminate between the two nearly equal signals. Detection limit for even the most favorable cases rarely exceeds 10^{-8} moles. But fluorometric instruments are limited only by the intensity of exciting light and the ability to detect low light levels. Under the ideal conditions the concentrations of 10^{-12} moles can be measured.

The decrease of the fluorescence intensity by interaction of the excited state of the fluorophore with its surroundings is known as quenching (not random process). The intermolecular electronic energy transfer is the possible way of RTIL fluorescence quenching:

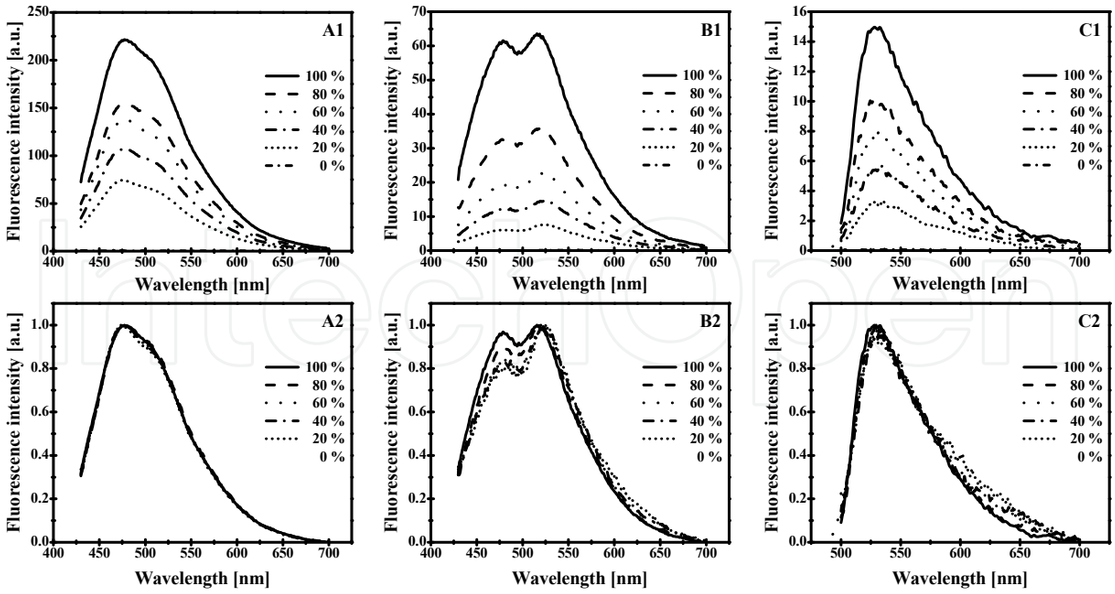


Fig. 8. The fluorescence emission spectra (A1) of binary solvent (A2 – normalized curves) (*IL4*), [C_8-C_1Im][BF_4] + DMF); the fluorescence emission spectra (B1) of all-*trans* β-carotene (B2 – normalized curves) 5 μmol in binary solvent and (C1) the 'pure' (corrected for fluorescence of ionic liquid) (C2 – normalized curves) fluorescence emission spectra (measured in the 10% step) of all-*trans* β-carotene in binary solvent mixture with different concentrations of RTIL (DMF signal is at the zero level), respectively; λ_{ex} = 413 nm; μ-cuvette.

RTIL* + β-carotene → RTIL + β-carotene*; where an excited molecule (RTIL*) transfers excitation energy to a quencher molecule β-carotene, causing deexcitation of RTIL and forming an excited quencher molecule, β-carotene*. If β-carotene* is a fluorescent species, its fluorescence, called sensitized fluorescence, can be detected. This is the phenomenon allowing observation of fluorescence from a molecule like β-carotene that may be difficult to excite directly because of the optically forbidden (for symmetry reason) singlet electronic states. The all-*trans* β-carotene in standard solvent, for example hexane, fluorescence quantum yield of electronic state S_2 is 2 x 10^{-4} (Sherve et al., 1991; Andersson, 1992) and of S_1 state is 4 x 10^{-6} (Wasielewski, 1986, 1989).

Figure	9A		9B		9C		9D	
	Slope	Slope [deg]	Slope	Slope [deg]	Slope	Slope [deg]	Slope	Slope [deg]
a	0.91	42	0.65	33	0.33	18	0.38	21
b	0.46	25	0.47	25	0.65	33	0.67	34
c	0.83	40	0.96	44	2.25	66	2.07	64

Table 3. The values of the slope for fitting linear dependence of fluorescence intensity on the percentage content of ionic liquid in binary solvent mixture ([C_8-C_1Im][BF_4] + DMF).

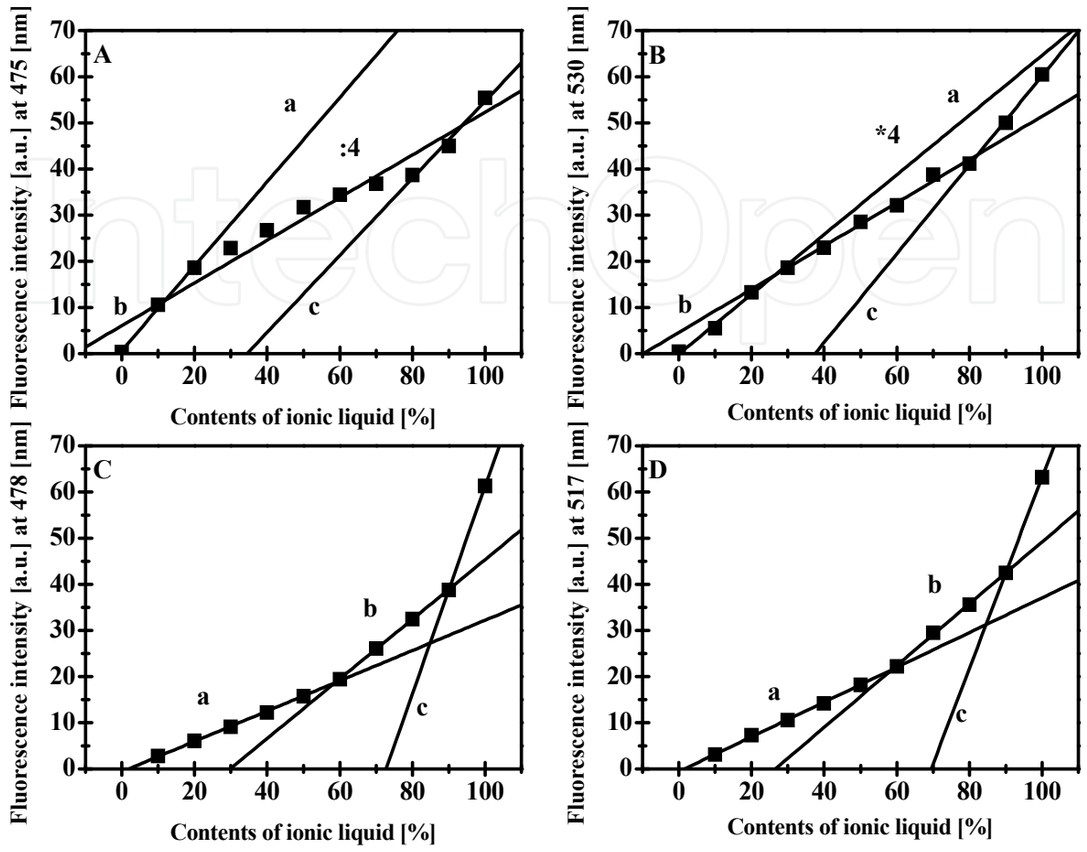


Fig. 9. The fluorescence emission intensity (A) of binary solvent (*IL4*), ([C_8-C_1Im][BF_4] + DMF) with different concentration of RTIL; (B) the 'pure' (corrected for fluorescence of ionic liquid) fluorescence emission spectra of all-*trans* β-carotene in binary solvent mixture (*IL4*), ([C_8-C_1Im][BF_4] + DMF). The fluorescence emission intensity (not corrected) of all-*trans* β-carotene in binary solvent for maxima: short wavelength (C) and long wavelength (D) with different concentration of RTIL. For all Figures. A, B, C, D measurements were done in the steps of 10% within concentration range of (0% - 100%) of RTIL; λ_{ex} = 413 nm; μ-cuvette.

Inner filter effects are often responsible for distorted emission spectra and nonlinear calibration curves between fluorescence intensity and fluorophore concentration. In a case of concentrated samples, in order to minimize or correct for IFE either instrumental or mathematical corrections can be done (Kao et al., 1998). Instrumental corrections are based on the observation that fluorescence intensity and fluorophore concentration are linear at low absorbance. In principle, any method that can lower the absorbance will reduce IFEs. Sample dilution (Guilbault, 1990; Lakowicz, 1983) is the most popular approach, but it may cause changes: in conformation, bonding, solvation, and the degree of association. Also other chemical events may alter absorption-fluorescence processes and, there by, introduce large unknown errors (Holland, 1977).

IFEs can distort fluorescence emission spectral profiles. Serious IFE will be indicated by changes in the shape of fluorescence spectra and position of max intensities in the

fluorescence measurements of the samples in standard and μ-cuvette. In a case of experiment in μ-cuvette, the PIFE is decreased because the excitation beam passes only through the 1 mm path instead of 10 mm. The SIFE is not negligible because optical density of the absorber (β-carotene) in emission wavelengths is not low. If samples absorb at both wavelengths: the fluorescence excitation and emission, the correction of the observed fluorescence for (IFE) is necessary (Tucker et al., 1992). This is the case of β-carotene in RTILs, the fluorescence excitation wavelength is at 413 nm and maximum of fluorescence emission at around 530 nm in standard cell.

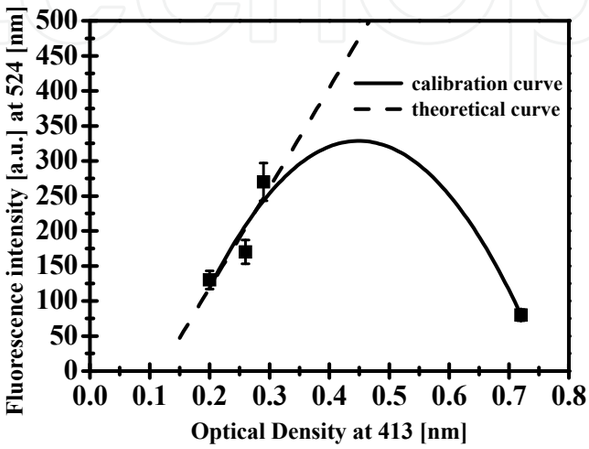


Fig. 10. The calibration curve of β-carotene in RTIL (*IL1*), 1-methyl-3-octyloxymethylimidazolium tetrafluoroborate) in 10 mm cell (right angle cell configuration).

If the calibration curve (Fig. 10) of the sample in 10 mm cuvette is perfectly linear this means that the (ε) molar extinction coefficient dependence on the (n) refractive index of the solution is negligible (Skoog & Leary, 1992). This is the case in our study where only up to OD = 0.2 the calibration curve is linear within experimental error.
The optical density (OD) of samples: β-carotene in RTILs and only RTILs at excitation and emission wavelengths are listed in Table 4.

RTILs	OD			
	β-carotene in RTIL		RTIL	
	413 [nm]	525 [nm]	413 [nm]	525 [nm]
IL1	0.28	0.04	0.00	0.00
IL2	0.26	0.04	0.00	0.00
IL3	0.25	0.06	0.00	0.00
IL4	0.10	0.04	0.63	0.06

Table 4. The sample optical density (OD) at excitation and emission wavelengths.

With temperature increased (in the physiological range: 283K and 313K, the fluorescence emission intensity decreased in both samples β-carotene in RTIL and also RTIL alone. Figures 11 (A-D) and 12 A & B show fluorescence emission spectra of RTIL and β-carotene in RTIL as a function of temperature.

The RTIL's fluorescence and absorption spectra changes induced by the temperature are correlated with the ionic liquid viscosity changes. The room temperature viscosity measurements of investigated RTILs are listed in Table 5.

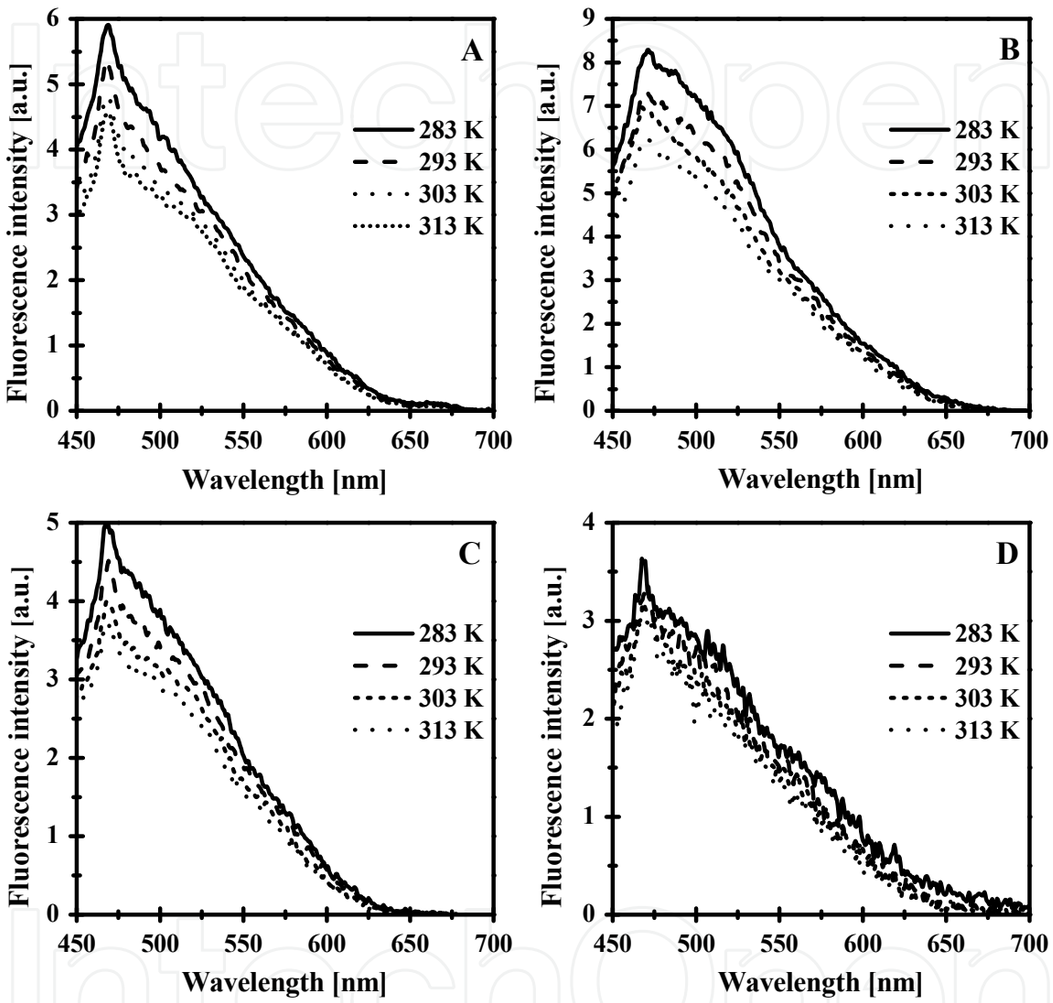


Fig. 11. Fluorescence emission spectra of: (A)- (*IL1*) $[C_8H_{17}OCH_2\text{-}C_1Im][BF_4]$; (B)- (*IL2*) $[C_6H_{13}OCH_2\text{-}C_1Im][(CF_3SO_2)_2N]$; (C)- (*IL3*) $[C_8H_{17}OCH_2\text{-}C_1Im][(CF_3SO_2)_2N]$; (D)- (*IL4*) $[C_8\text{-}C_1Im][BF_4]$ (μ-cuvette) as a function of temperature.

RTILs	Viscosity [cP]	Reference data
$[C_8H_{17}OCH_2\text{-}C_1Im]$ $[BF_4]$	574	
$[C_8H_{17}OCH_2\text{-}C_1Im]$ $[(CF_3SO_2)_2N]$	105	
$[C_6H_{13}OCH_2\text{-}C_1Im]$ $[(CF_3SO_2)_2N]$	87	
$[C_8\text{-}C_1Im]$ $[BF_4]$	420	439 (Seddon et al., 2002)

Table 5. The viscosity (error 2%) of RTILs.

The fluorescence quantum yield of all-*trans* β-carotene in the investigated ionic liquids are shown in Figure 12.

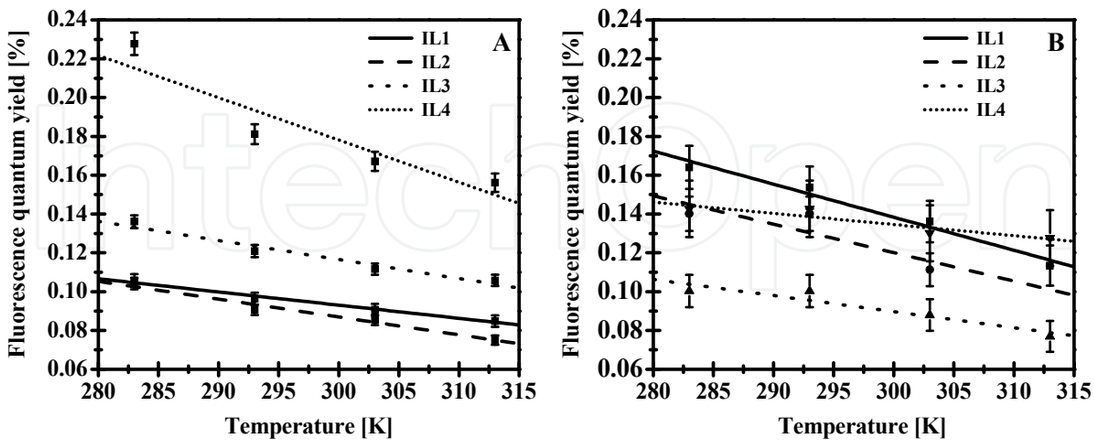


Fig. 12. The fluorescence quantum yield of all-*trans* β-carotene in: *IL1* - $[C_8H_{17}OCH_2\text{-}C_1Im][BF_4]$; *IL2* - $[C_6H_{13}OCH_2\text{-}C_1Im][(CF_3SO_2)_2N]$; *IL3* - $[C_8H_{17}OCH_2\text{-}C_1Im][(CF_3SO_2)_2N]$; *IL4* - $[C_8\text{-}C_1Im][BF_4]$: (A) - before correction for fluorescence ionic liquid; (B)- 'pure' all-*trans* β-carotene spectra corrected for fluorescence of ionic liquid.

In order to check fluorescent impurities of the sample the fluorescence emission spectra with different excitation wavelengths ought to be measured. The fluorescence maxima of the RTILs investigated by us based on imidazolium are strongly dependent on the excitation wavelengths similarly as was found by other authors (Paul & Samanta, 2006). In the present study we focus on four RTILs with different combination of cations or anions (*see* Scheme 1). Special care was taken for the purification of the synthesized ionic liquids.

The dependence of fluorescence emission spectra of all-*trans* β-carotene on excitation wavelength is presented in Figure 13.

There exist two sets of data (Figures 14 A and B): one with max around 400 nm and second with max shifted toward longer wavelength with increasing excitation wavelength in the range between 350 nm and 450 nm. The RTILs based on imidazolium are not as transparent as commonly has been believed. Also an excitation wavelength dependent fluorescence effect known as 'red edge effect' is observed. The various energetically different associated species in RTILs are responsible for this 'red tail'.

4. Conclusion

The $[BF_4]^-$ and $[(CF_3SO_2)_2N]^-$ based imidazolium ionic liquids have non-negligible absorption in the UV-VIS region with the absorption red tail extending far into the visible region. Such effect is also observed in very carefully purified RTILs. Inner filter effects are responsible for distorted emission spectra and nonlinear calibration curves between fluorescence intensity and fluorophore concentration. In a case of samples like RTILs in order to minimize IFE the μ-cell ought to be used. Other methods may cause changes in the nanostructure of ions and influence the intensity and shape of the fluorescence spectra.

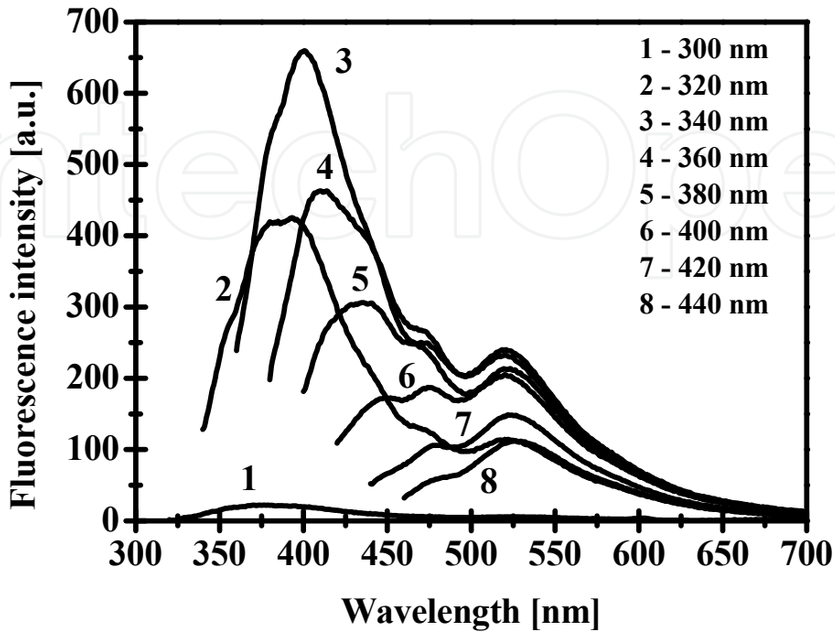


Fig. 13. Fluorescence emission spectra of all-*trans* β-carotene; c = 5 [μM] in (*IL1*), $C_8H_{17}OCH_2$-C_1Im][BF_4]; 10 mm cuvette; as a function of excitation wavelength.

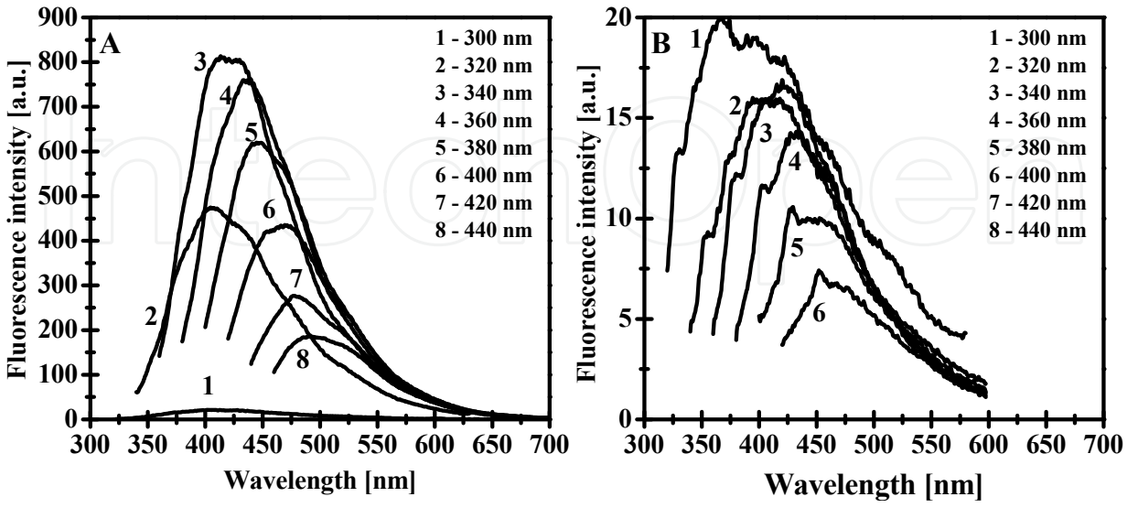


Fig. 14. Fluorescence emission spectra of (*IL1*), [$C_8H_{17}OCH_2$-C_1Im][BF_4] in: (A) -10 mm standard cuvette and (B) - μ–cuvette, as a function of excitation wavelength.

5. Acknowledgements

Acknowledgement is made to project DS. 62-176/2011.
ISBN 978-1-4051-3891-8

6. References

Albani, J.R. (2007). *Principles and Applications of Fluorescence Spectroscopy*, Wiley-Blackwell, ISBN 978-1-4051-3891-8, Malaysia.

Andersson, P.O., Gillbro, T.A., Asato, E., & Liu, R.S.H. (1992). Dual singlet state emission in a series of mini-carotenes. *Journal of Luminescence*, Vol. 51, No. 1-3, pp. 11- 20, ISSN 0022-2313.

Bialek-Bylka, G.E., Pawlak, K., Jazurek, B., Skrzypczak, A., & Koyama, Y. (2007). Spectroscopic properties and temperature induced electronic configuration changes of all- *trans* and 15- *cis* β-carotenes in ionic liquids. *Photosynthetica*, Vol. 45, No. 2, pp. 161-166, ISSN 0300-3604.

Bialek-Bylka, G.E., Kakitani, Y., Li, Ch., Koyama, Y., Kuki, M., Yamano, Y., & Nagae, H. (2008). Excitation followed by stimulated-emission from diabatic levels in all-*trans* and 15-*cis*-β-carotenes: Effects of molecular symmetry and solvent polarity. *Chemical Physics Letters,* Vol. 454, No. 4-6, pp. 367-373, ISSN 0009-2614.

Earle, M.J., Gordon, Ch.M., Pletchkova, N.V., Seddon, K.R., & Welton, Th. (2007). Decolorization of Ionic Liquids for Spectroscopy. *Analytical Chemistry,* Vol. 79, No. 2, pp. 758-764, ISSN 0003-2700.

Gordon, C.M., McLean, A.J., Muldoon, M.J., & Dunkin I.R. (2003). Diffusion-Controlled Reactions in Room Temperature Ionic Liquids, *Proceedings of Ionic Liquids as Green Solvents: Progress and Prospects-224th American Chemical Society National Meeting*, ISBN 9780841219618, Boston, August 2002.

Guilbault, G.G. (1990). *Practical fluorescence* (2nd. edition), Mercel Dekker Inc., ISBN 0824783506, New York.

Holland, J.F., Teets, R.E., Kelly, P.M., & Timnick, A. (1977). Correction of right-angle fluorescence measurements for the absorption of excitation radiation. *Analytical Chemistry*, Vol. 49, No. 6, pp. 706-710, ISSN 0003-2700.

Ingle, J.D., & Crouch, S.R. *Spectrochemical Analysis*, Prentice-Hall Inc., ISBN 0-13-826876-2, Upper Saddle River.

Kao, S., Asanov, A.N., & Oldham, P.B. (1998) A Comparison of Fluorescence Inner Filter Effects for Different Cell Configurations. *Instrumentation Science & Technology*, Vol. 26, No. 4, pp. 375-387, ISSN 1073-9149.

Koel, M. (2008). *Ionic Liquids in Chemical Analysis*, CRC Press, ISBN 1-4200-4646-2, Boca Raton.

Lakowicz, J.R. (1983). *Principles of fluorescence spectroscopy* (1st edition), Plenum Press, ISBN 0306412853, New York.

Lakowicz, J.R. (2006). *Principles of fluorescence spectroscopy* (3rd edition), Springer, ISBN 0387312781, Singapore.

Li, H., & Hu, Y. (2007). Spectroscopic investigation of inner filter effect by magnolol solutions. *Spectrochimica Acta Part A: Molecular and Biomolecular Spectroscopy*, Vol. 68 No. 5, pp. 1263-1268, ISSN 1386-1425.

Lidke, D., Nagy, P., Barisas, B., Heintzmann, R., Post, J., Lidke, K., Clayton, A., Arndt-Jovin, D., & Jovin, T. (2003). Imaging molecular interactions in cells by dynamic and static fluorescence anisotropy (rFLIM and emFRET). *Biochemical society transactions*, Vol. 31, No. 5, pp. 1020-1027, ISSN 0300-5127.

Mandal, P.K., Saha, S., Karmakar, R., & Samanta, A. (2006). Solvation dynamics in room temperature ionic liquids: Dynamic Stokes shift studies of fluorescence of dipolar molecules. *Current Science*, Vol. 90, No. 3, pp. 301-310, ISSN 0011-3891.

Moss, T., & Leblanc, B. (2009). *DNA-Protein Interactions: Principles and Protocol* (3rd edition), Humana Press, ISBN 1603270140, Dordrecht Heidelberg London New York.

Pawlak, K., Skrzypczak, A., & Bialek-Bylka, G.E. (2009). Reichardt's dye as sensor material detected oxymethyl group in the cation part of imidazolium ionic liquid structure. *Journal of Engineering and Applied Sciences*, Vol 4, No. 7, pp. 71-74, ISSN 1819-6608.

Paul, A., & Samanta, A. (2006). Optical absorption and fluorescence studies on imidazolium ionic liquids comprising the bis(trifluoromethane - sulphonyl)imide anion. *Journal of Chemical Sciences* Vol. 118, No. 4, pp. 335-340, ISSN 0974-3626.

Pernak, J., Czepukowicz, A., & Pozniak, R. (2001). New Ionic Liquids and Their Antielectrostatic Properties. *Industrial & Engineering Chemistry Research*, Vol. 40, No. 11, pp. 2379-2383, ISSN 0888-5885.

Seddon, K., Stark, A., & Torres, M.J. (2002). Viscosity and Density of 1-Alkyl-3-methylimidazolium Ionic Liquids, *Proceedings of Clean Solvents: Alternative Media for Chemical Reactions and Processing*, ISBN 9780841219182, Washington DC, August 2000.

Shreve, A.P., Trautman, J.K., Owens, T.G., & Albrecht, A. C. (1991). A femtosecond study of electronic state dynamics of fucoxanthin and implications for photosynthetic carotenoid-to-chlorophyll energy transfer mechanisms. *Chemical Physics*, Vol. 154, No. 1, pp. 171-178, ISSN 0301-0104.

Skoog, D. A., & Leary, J. J. (1992). *Principles of Instrumental Analysis* (5th edition), Saunders College Publishing, ISBN 0030020786, Madrid.

Tucker, S.A., Amszi, V.L., & Acree, W. E. (1992). Primary and secondary inner filtering. Effect of $K_2Cr_2O_7$ on fluorescence emission intensities of quinine sulfate. *Journal of Chemical Education*, Vol. 69, No. 1, pp. A8, ISSN 0021-9584.

Wasielewski, M.R., & Kispert, L.D. (1986). Direct measurement of the lowest excited singlet state lifetime of all-*trans*-β-carotene and related carotenoids. *Chemical Physics Letters*, Vol. 128, No. 3, pp. 238-243, ISSN 0009-2614.

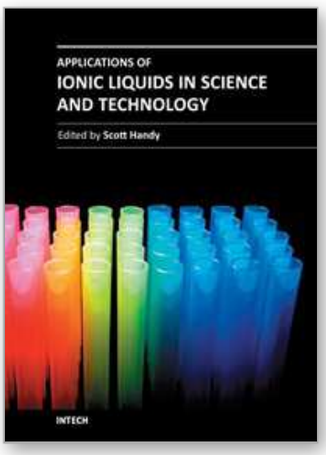
Wasielewski, M.R., Johnson, D.G., Bradford, E. G., & Kispert, L.D. (1989). Temperature dependence of the lowest excited singlet-state lifetime of all-*trans*-β-carotene and

fully deuterated all-*trans*-β-carotene. *The Journal of Chemical Physics* Vol. 91, No.11, pp. 6691-6697, ISSN 0021-9606.

Wasserscheid, P., & Welton, T. (2008). *Ionic liquids in synthesis* (2nd edition), Vch Verlagsgesellschaft Mbh, ISBN 978-3-527-31239-9, Weinheim.

IntechOpen

IntechOpen



Applications of Ionic Liquids in Science and Technology

Edited by Prof. Scott Handy

ISBN 978-953-307-605-8
Hard cover, 516 pages
Publisher InTech
Published online 22, September, 2011
Published in print edition September, 2011

This volume, of a two volume set on ionic liquids, focuses on the applications of ionic liquids in a growing range of areas. Throughout the 1990s, it seemed that most of the attention in the area of ionic liquids applications was directed toward their use as solvents for organic and transition-metal-catalyzed reactions. Certainly, this interest continues on to the present date, but the most innovative uses of ionic liquids span a much more diverse field than just synthesis. Some of the main topics of coverage include the application of RTILs in various electronic applications (batteries, capacitors, and light-emitting materials), polymers (synthesis and functionalization), nanomaterials (synthesis and stabilization), and separations. More unusual applications can be noted in the fields of biomass utilization, spectroscopy, optics, lubricants, fuels, and refrigerants. It is hoped that the diversity of this volume will serve as an inspiration for even further advances in the use of RTILs.

How to reference
In order to correctly reference this scholarly work, feel free to copy and paste the following:

Krzysztof Pawlak, Andrzej Skrzypczak and Grazyna E. Bialek-Bylka (2011). Inner Filter Effect in the Fluorescence Emission Spectra of Room Temperature Ionic Liquids with-β-Carotene, Applications of Ionic Liquids in Science and Technology, Prof. Scott Handy (Ed.), ISBN: 978-953-307-605-8, InTech, Available from: http://www.intechopen.com/books/applications-of-ionic-liquids-in-science-and-technology/inner-filter-effect-in-the-fluorescence-emission-spectra-of-room-temperature-ionic-liquids-with-caro

INTECH
open science | open minds

InTech Europe
University Campus STeP Ri
Slavka Krautzeka 83/A
51000 Rijeka, Croatia
Phone: +385 (51) 770 447
Fax: +385 (51) 686 166
www.intechopen.com

InTech China
Unit 405, Office Block, Hotel Equatorial Shanghai
No.65, Yan An Road (West), Shanghai, 200040, China
中国上海市延安西路65号上海国际贵都大饭店办公楼405单元
Phone: +86-21-62489820
Fax: +86-21-62489821

© 2011 The Author(s). Licensee IntechOpen. This chapter is distributed under the terms of the Creative Commons Attribution-NonCommercial-ShareAlike-3.0 License, which permits use, distribution and reproduction for non-commercial purposes, provided the original is properly cited and derivative works building on this content are distributed under the same license.

IntechOpen

IntechOpen